

Thermodynamics of phyllosilicates and low temperature thermometry

*Olivier Vidal*¹, *Armelle Baldeyrou*², *Benoit Dubac*¹, *Vincent DeAndrade*³, *Michel Jullien*⁴
*and B. Lanson*¹

¹ LGCA. LGIT. Université Joseph Fourier. Grenoble. olivier.vidal@ujf-grenoble.fr

² LGS. Université Louis Pasteur. Strasbourg.

³ ESRF. Grenoble.

⁴ CEA. Cadarache.

Introduction

Temperature (T) and pressure (P) conditions of medium- to high-grade rocks metamorphosed at T above about 400°C are estimated using equilibrium thermodynamics. In principle, the same approach could be used for low-grade rocks (early diagenesis to metamorphic conditions), where typical mineral evolutions such as the transitions from smectite → illite/smectite → illite → muscovite are observed with increasing T, which are associated with continuous change of mineral composition (e.g. chlorite). However, application of classical thermometric approaches to low-T rocks is limited by several factors:

1) In contrast to metamorphic rocks, low variance parageneses are often difficult to identify, and a strong heterogeneity of mineral compositions is generally observed. This compositional heterogeneity raises the question of which minerals and compositions should be used together to estimate T conditions.

2) Temperature estimates in low-grade rocks must have low uncertainties, typically less than 50°C. This requires well constrained and reliable thermodynamic data and solid solution models, which are lacking for clay minerals. Even the thermodynamic status of clay and interstratified minerals is still unclear. Moreover, most available thermodynamic properties for clays are based on solubility experiments (sometimes unreversed) or they are predicted using various algorithms. Owing to the low kinetics of reaction at low-temperature, experimental reversals of equilibrium reaction cannot be achieved. This limits the possibility of deriving internally consistent thermodynamic data and solid-solution models. Moreover, extrapolation towards high temperature (HT) domains and the compatibility of the existing thermodynamic data with those of minerals stable at higher temperatures is not made. Last, the non-ideal behaviour of solid-solutions observed in the case of HT phyllosilicates is generally neglected for low-T phyllosilicates, and thermodynamic modelling of dehydration with temperature is not always addressed.

We present some recent advances made in the field of metamorphic thermobarometry, and experimental approaches that can help to solve some of the problems outlined above.

From mineral composition to temperature estimates using a multi-equilibrium approach

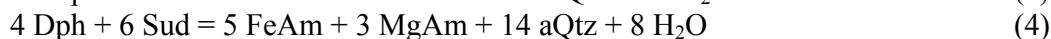
Chlorites

Cathelineau and Nieva (1985) showed that the amount of Al^{IV} in chlorite decreases and the amount of vacancy increases with decreasing temperature. They proposed the first empirical thermometer based on the Al^{IV} content of chlorite. The composition-temperature trends observed by Cathelineau and Nieva (1985) have a thermodynamic explanation, and they can be modelled using a chlorite solid-solution model with a set of 3 chlorite end-members (Mg-sudoite, Clinochlore, Mg-amesite) of known thermodynamic properties (Vidal et al., 2001, 2005, 2006).

In presence of quartz, the vacancies and Al^{IV} contents of chlorite can be modelled by the following equilibrium (Vidal et al., 2001):



At fixed water activity, the temperature location of E1 depends on the proportions and therefore activities of Clin, Sud and Am end-members components in chlorites. An increase of sudoite proportion (increase of vacancies) at given Clin/Am proportion leads to a shift of E1 towards low temperature, whereas an increase of the Am proportion (increase of Al^{IV}) leads to a shift toward high temperature. An important point here is that an equilibrium temperature can be calculated for the high variance paragenesis made of chlorite + quartz in presence of water ($v = 4$ in the system $\text{FeO-MgO-Al}_2\text{O}_3\text{-SiO}_2\text{-H}_2\text{O}$). This is possible because equilibrium (E1) can be written when using the sudoite, Mg-amesite and clinochlore end-members to describe the Tschermack and di-trioctahedral substitutions. By comparison to empirical Al^{IV} -T relations, the thermodynamic formulation is not limited to the temperature range and rock composition at which the thermodynamic properties were constrained. It is expected to give reliable results over a wider range of physicochemical conditions of crystallisation. To express any chlorite composition in the FMASH system ($Si < 3$ a.p.f.u), additional end-members are required (Daphnite, Fe-amesite and Fe-sudoite). Due to the lack of experimental data on the stability of Fe-sudoite and on the possible ordering of Fe and Mg, substitutions in chlorite were modelled by Vidal et al. (2001, 2005 and 2006) with the 5 end-members clinochlore (Clin), Fe- and Mg-amesite (FeAm and MgAm), daphnite (Daph) and Mg-sudoite (Sud). Using these end-members, three additional reactions can be written for chlorite-quartz-water assemblages:



Vidal et al. (2005, 2006) proposed to adjust the amount of Fe^{3+} in chlorite, which affect the activity of all end-members, to obtain convergence of (E1) to (4). A simultaneous estimation of Fe^{3+} in chlorite and equilibrium temperature for the Chl-Qtz- H_2O assemblage could be done at given pressure and a_{H_2O} using this approach, but it remains to be tested in details against independent measurements.

Since one temperature can be estimated for any chlorite composition, the multi-equilibrium approach can be used to calculate temperature maps at the thin section scale, which highlight the link between mineral reactivity and deformation. Application examples by DeAndrade et al. (2006), Vidal et al. (2006) and Yamato et al. (2007) indicate that different temperatures ranging from 500 to 150°C can be obtained from the same thin section (Figure 1). This extend of the range of temperature is proportional to the heterogeneity in chlorite composition, which is either a controlled by the availability of the constituent elements during its growth (control by the local bulk rock and/or fluid composition), and the metastable coexistence of different chlorite generations formed at different P-T conditions. The mapping approach clearly indicates that the coexistence of chlorite grains with different compositions is **not** a argument for the lack of thermodynamic equilibrium at low temperature. The coexistence of chlorites with different compositions simply indicates that equilibrium is achieved locally, and that the zones where equilibrium is achieved are the most deformed ones. A lower kinetic of reaction has the effect of decreasing the size of domains in thermodynamic equilibrium, but thermodynamic equilibrium can still be achieved at very low temperature.

A similar approach coupling multi-equilibrium thermodynamics with quantitative maps of composition could be used for other phyllosilicates showing several substitutions (e.g. Fe-Mg, di-

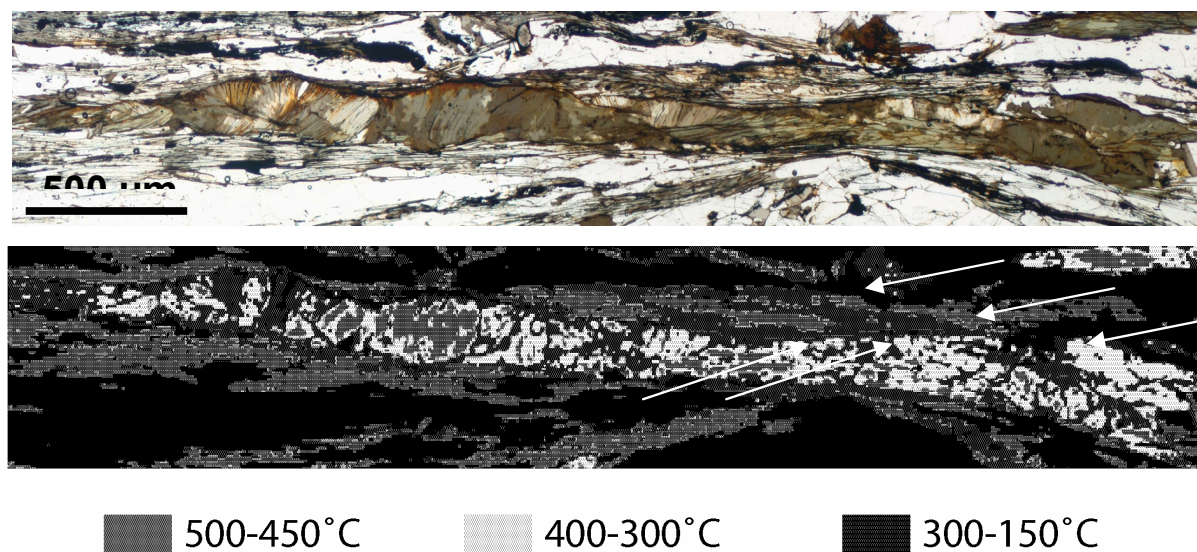


FIGURE 1. *Top: optical micrograph of a thin section showing a chlorite crystallization tail surrounded by micas on both sides. Bottom: calculated temperature map. One temperature is calculated for each chlorite and mica pixels (5 μ m diameter and 5 μ m step). The arrows show two parallel shear bands crosscutting an older mica aggregate and running through the chlorite crystallisation tail. Calculated temperatures within this shear bands are about 200°C, whereas the surrounding mica formed at $T > 450^\circ\text{C}$. This shows that mineral reactivity is activated by local deformation, which allows local equilibration of the chlorite and mica compositions at low temperature. Adapted from Vidal et al. (2006).*

trioctahedral, Tschermack), which is the case of micas and clay minerals in low-T rocks. However, this will be possible at the condition that:

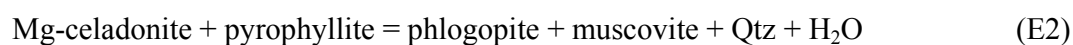
1) well constrained standard state and solid solution thermodynamic data are available. In the case of chlorite, the calculated temperatures are very sensitive to the small changes in composition and activities of end-members. Another conclusion that can be drawn from the chlorite example is that ideal activity models are probably not appropriate for low-temperature phyllosilicates. For instance, the di-trioctahedral sudoite and tri-trioctahedral chlorites end-members coexist as individual phases in aluminous pelites. This indicates unmixing of these phases and therefore a non-ideal solid solution model. The same unmixing of dioctahedral and trioctahedral end-members is a general feature of all phyllosilicates (e.g. muscovite-biotite, beidellite/montmorillonite-saponite, talc-pyrophyllite, etc), and it should be taken into account for low-T phyllosilicates.

2) good quality quantitative maps of composition can be measured for very fine-grained samples with a sufficient spatial resolution.

These two points are addressed in the following sections.

Micas

Like chlorites, micas also show Fe-Mg, di-trioctahedral and Tschermak substitutions, and a pyrophyllitic substitution responsible for the incorporation of vacancies in the interlayer position. The composition of mica can be modelled with the muscovite, Fe- and Mg-celadonite, pyrophyllite and phlogopite, annite end-members. With these end-members, equilibrium similar to E1 can be written for micas:



In contrast to E1 that mostly depends on temperature, E2 has a flatter slope (about 20bar/ $^\circ\text{C}$) in a P-T diagram, with Mg-Cel + Prl on the low temperature, high pressure side. At constant

pressure, E2 indicates that in agreement with the observations of Kossovskaya and Drits (1970), the Al content of tetrahedral sheet of K-white mica increases with increasing metamorphic grade (increase of phlogopite and muscovite activities). The amount of vacancies (pyrophyllite activity) is predicted to increase with decreasing temperature, as observed in nature. However, a careful use of these trends is necessary because at constant pressure, there is a competition effect between the di-trioctahedral and Tschermack substitutions. A decrease of Al^{IV} and increase of $(Mg + Fe^{2+})$ due to the Tschermack substitution (increase of Mg-celadonite proportion) can be counterbalanced by an increase of the trioctahedral end-members proportions. The amount of trioctahedral end-member in dioctahedral mica from metamorphic rocks has been shown to be higher at high temperature and pressure than at medium temperature. This is compatible with an increase of the miscibility (solvus narrowing) with increasing temperature. The same observation has been made from HP-HT experimental studies (Green 1981). However, Leoni et al. (1998) found that the amount of trioctahedral end-member in dioctahedral mica is also significant in low grade rocks. The same authors concluded that the extent of the di-trioctahedral substitution in low-T mica depends primarily on bulk rock chemistry rather than on metamorphic conditions. However, Vidal et al. (2006) observed that micas crystallizing in late shear bands at low temperature have a higher octahedral occupancy than HT-HP micas coexisting in the same thin section (Figure 1). In this particular case, the effect of bulk rock composition should be low.

These basic observations suggest that the octahedral occupancy, the $(Mg + Fe)$, Al^{IV} or the vacancy contents of mica cannot be used individually as indicators of temperature. However, as for chlorites, temperature estimates can be made at given pressure when all contents and possible substitutions are considered at the same time, through an equilibrium of the type E2.

Toward a (unique) solid-solution model for K-white mica, pyrophyllite, illite and K-beidellite...

Smectite, illite and I/S are obviously important minerals when dealing with very low-T rocks. On a chemical point of view, illite is similar to dioctahedral micas with a deficit of interlayer cation, and it can be partially hydrated. Loucks (1991) showed that with decreasing temperature, the apparent vacancies of dioctahedral mica are partly filled by either neutral water molecules or hydronium cations. He proposed to use the additional end-members hydronium-muscovite and hydrated-pyrophyllite to model the composition of LT mica. Using thermodynamic arguments, Loucks (1991) anticipated that these end-members could allow modelling of the partial hydration of illite at low temperature and its dehydration with increasing temperature. This statement can probably be extended to smectites. In the past, dioctahedral smectites of Si-Al-K proportions intermediate between muscovite and pyrophyllite (K-beidellite) have been modelled as a solid solution between pyrophyllite and muscovite (e.g. Giggenbach, 1984). This approach is appropriate to explain the Si, Al, K and apparent interlayer vacancies of dioctahedral smectites. However, there is a very wide miscibility gap between muscovite and pyrophyllite, which has been used by Jiang et al. (1990) as an argument for the metastability of beidellite compared to the assemblage muscovite + pyrophyllite. This argument is specious and the conclusion of Jiang et al. (1990) is probably false because beidellite is a hydrated mineral that cannot be modelled as a linear combination of pyrophyllite and muscovite dehydrated end-members. Additional (theoretical) end-members are required, such as the hydrated-pyrophyllite (PrIH: $Si_4Al_2O_{10}(OH)_2.nH_2O$) and hydronium-muscovite (MuscHyd: $Si_3Al_3O_{10}(OH)_2.H_3O^+$) end-members proposed by Loucks (1991), or/and hydrated-muscovite (MuscH: $Si_3Al_3O_{10}(OH)_2.nH_2O$) proposed by Ransom and Helgeson (1995). With the four end-members (Musc, MuscHyd and/or MuscH, PrI and PrIH), illite and smectite compositions can be modelled in the $SiO_2-Al_2O_3-K_2O-H_2O$ (KASH) chemical system, but thermodynamic modelling has never been achieved yet.

We have conducted this thermodynamic modelling of the smectite-illite-musc + pyrophyllite compatibility and stability relations in the KASH systems, which is the first step towards more complex compositions observed in nature. For reasons of simplicity, the hydrated-muscovite (MuscH) end-member proposed by Ransom and Helgeson (1995) was used instead of MuscHyd end-members, and fully PrlH and MuscH was assumed to contain $n = 4$ mole H_2O (instead of 4.5 after Ransom and Helgeson, 1995). The dehydration isopleths of MuscH reported by Ransom and Helgeson (1995) were reproduced with $\delta S^{\circ}hyd-K = (S^{\circ}MuscH - S^{\circ}Musc) = 220 \text{ J/mol/K}$, $\delta V^{\circ}hyd-K = 6.88 \text{ cm}^3$, $\delta H^{\circ}hyd-K = -1160.74 \text{ kJ/mol}$ and $WMusc-MuscH = 10 \text{ kJ}$. The same “ δ ” values were used to estimate the standard state properties of PrlH, and the Margules parameter $WPrIH-Prl$ was adjusted in order to locate the $Kln-PrlH$ transition between 150 and 200°C. With these parameters, it is possible to calculate the stable phyllosilicate compositions and their evolution with temperature for bulk compositions intermediate between pyrophyllite + excess water and muscovite + excess water. The stable mineral assemblage and mineral compositions were calculated as a function of temperature by energy minimizing with the softwares *theriak* and *domino* (de Capitani, 1997). Results are shown in Figure 2a. At low temperature, almost fully hydrated smectite is stable. Its composition is controlled by the bulk system composition and complete solid solution is observed from the (Prl + PrlH) to (Musc + MuscH) compositions. With increasing temperature, unmixing occurs and two phases are stable together, one rich in (Prl \pm PrlH) and the other rich in (Musc \pm MuscH).

These phases have compositions corresponding to that of smectite and illite, respectively. Progressive dehydration with increasing temperature is predicted by a decrease of the relative proportion of (PrlH + MuscH) in both smectite and illite. However, dehydration is more rapid with increasing temperature for illite than for the smectite, as it is observed in nature. At 300°C, smectite and illite are almost completely dehydrated, and their composition is close to that of Prl and Musc.

Obviously, these calculations made in the KASH system are of limited interest, and a more complex formalism is needed to reproduce the clay compositions observed in natural rocks. However, several points are worth to note:

1) The relative stabilities and compatibility relations among smectite, illite, muscovite and pyrophyllite can be modelled with a unique solid solution model. At low temperature, hydrated clay minerals of Si/Al/K proportions between Musc and Prl are more stable than these end-members. Our modelling predicts an “inversed solvus”, i.e. the miscibility between (Musc + MuscH) and (Prl + PrlH) increases with decreasing temperature (Figure 2a). This resolves the ambiguity concerning the apparent metastability of beidellite when modelled with Prl and Musc end-members (Jiang et al., 1990). The successive assemblages smectite \rightarrow smectite + illite \rightarrow pyrophyllite + muscovite observed in natural rocks are reproduced by energy minimizing.

2) At fixed bulk composition, the composition of smectite and illite is predicted to vary with temperature. This concerns the amount of water that decreases with increasing temperature, but also the Si/Al/K ratio. Interlayering of illite and smectite cannot be modelled with our approach yet, but the composition of the illite and smectite layers in I/S should also change with varying temperature. To our knowledge, this has never been observed in natural rocks.

3) Dehydration is more rapid in the 100 to 200°C range of temperature than at lower and higher temperature. This is consistent with the staircase shape of the dehydration curves obtained during heating of smectite. However, only one dehydration step predicted by the model at about 150°C, which is not consistent with the multi-step dehydrations corresponding to the 3 \rightarrow 2 \rightarrow 1 \rightarrow 0 level H_2O observed on natural samples.

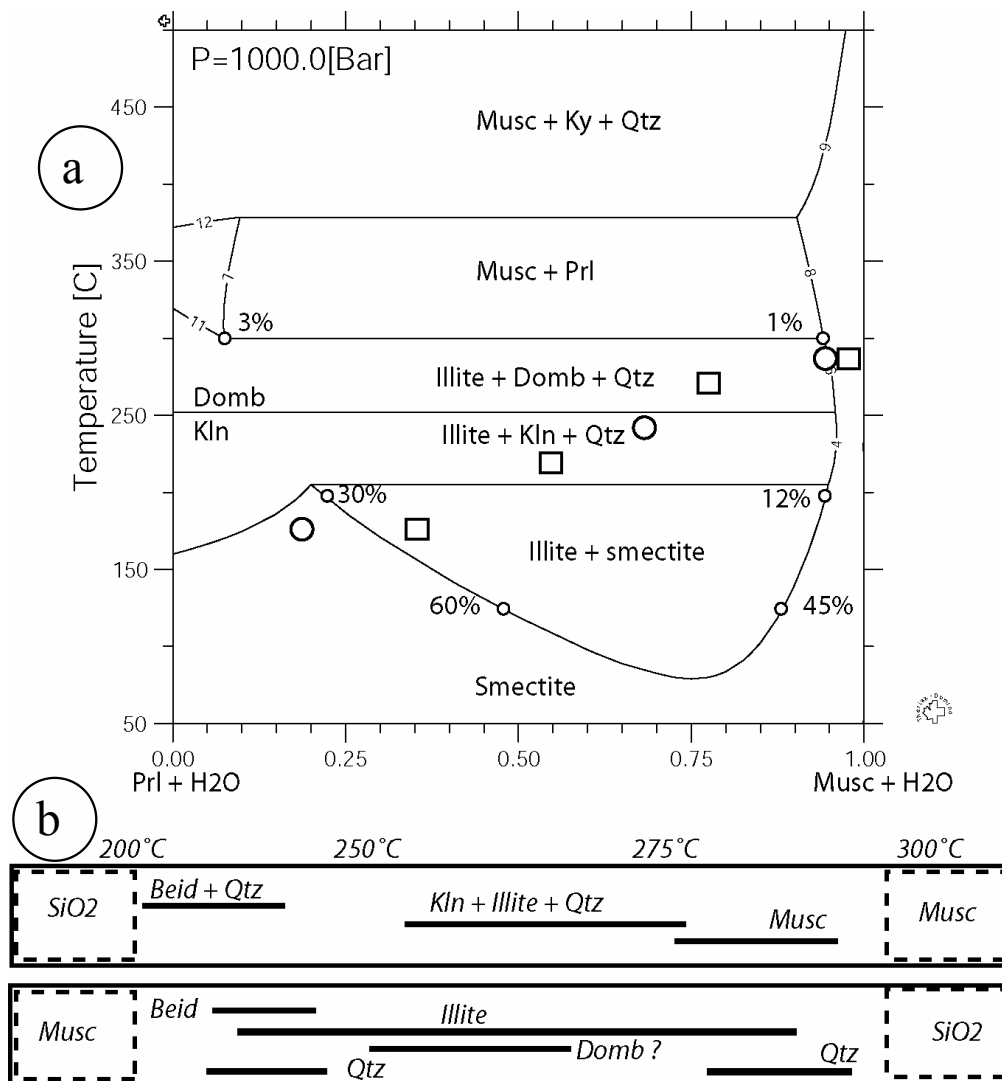


FIGURE 2. a) Calculated T -composition phase diagram at 1 kbar, for composition between $Prl + PrlH + H_2O$ and $Musc + MuscH + H_2O$. The numbers refer to the molar fraction (%) of hydrated end-members ($PrIH + MuscH$) in the stable phases. The circles and squares show the evolution of system composition along the tubes in experiment 1) and 2), respectively (Figure 2b). b) Results of experiments with $Musc$ and Qtz starting gels. The material is sealed in perforated capsules located at the extremities of a tube filled with water. The tube is placed in a strong thermal gradient. Two experiments (1 and 2) are performed with opposite capsule locations.

Experimental constrains on the T -composition-mineralogy relationships of low temperature phyllosilicates.

Numerous thermodynamic models and data are available for clays minerals, but none of them are based on reactions bracketing, because the reaction kinetics is too sluggish at low-temperature. They are generally constrained by solubility experiments, for which the fluid composition is analysed after quenching. A drawback of the solubility experiments is the possible lack of equilibrium between fluid and minerals, or/and the possible crystallization of undetected phases buffering the fluid composition. For this reason, we tried to obtain new experimental results in a system under thermodynamic disequilibrium, which is a driving force for fluid-solid reaction and mass transport.

Experimental procedure and compositions

Vidal et al. (1997) suggested that experiments conducted under a thermal gradient might be used to constrain the relative thermal stability of low-temperature phyllosilicates such as clay minerals as well as their composition-temperature dependencies. The advantage of this experimental approach is that the newly formed products are separated from the starting material. This avoids any ambiguity in the identification and analysis of the reaction products. Tube-in-tube experiments similar to those described by Vidal (1997) were conducted in the $K_2O-Al_2O_3-SiO_2-H_2O$ (KASH) chemical system, in order to constrain the relative stability and composition-temperature relations among smectite, illite and mica at different level of SiO_2 , K_2O and Al_2O_3 saturation.

Starting amorphous mixtures of various compositions were sealed in capsules with drilled walls. Two capsules were placed at the end(s) of a 15 cm gold tube containing only water. The tube was welded shut and placed in a cold seal autoclave at 1 kbar, under a strong thermal gradient (from 350°C at the hot extremity to 200°C at the cold extremity). After three months, the neoformed phases on the tube walls were observed and analyzed with a scanning electron microscope. When it was possible, the products were collected for XRD or TEM characterisation. In order to study the effect of the bulk system composition, the experiments were conducted in quartz-saturated and quartz undersaturated systems. In an attempt to reverse the T-stability-composition experimental results, two experiments were realized for each bulk system compositions, in which the location of the starting (cold and hot extremities) were reversed.

Results and discussion

The experimental results are shown in Figs 2b and 3b. At Qtz-saturated conditions (muscovite and quartz gels in the capsule, Figure 2b), beidellite \pm Qtz crystallized at 200 to 250°C, illite \pm Kln \pm Qtz at 250-350°C, and muscovite at T 300-350°C. Illite-smectite interlayering has not been observed. At Qtz undersaturated conditions (muscovite + kaolinite gels, Figure 3b), muscovite \pm Al-dombassite was observed at the hot extremity, illite + Al-dombassite + kaolinite at intermediate position, and kaolinite \pm K-rich smectite at T < 230°C.

Similar crystallization sequences were obtained when changing the relative position of the starting products (LT or HT sides of the tube). Therefore, the temperature crystallization sequences were reversed for all bulk system composition. The control by the bulk system composition of the crystallizing phases is evident, but for a given bulk composition, the crystallisation sequences give information about the relative stability of the newly formed products. For instance, the transition smectite \rightarrow illite \rightarrow muscovite observed in nature with increasing temperature has been reproduced experimentally. A general feature is the crystallisation of the most aluminous phases at the cold extremity, and K-rich phases at the hot extremity. Additional experiments conducted in presence of Mg show that these observations can be extended to other chemical compositions. These additional experiments in presence of Mg show that trioctahedral and dioctahedral smectites coexist in the intermediate position of the quartz-bearing experiments. This indicates a lack of miscibility between hydrated-talc (stable at HT) and hydrated-pyrophyllite (LT) smectite compositions. The formation of dioctahedral phyllosilicate at the cold extremity, followed by di-trioctahedral and then trioctahedral phyllosilicates at the hot extremity seems to be also systematic.

The experimental results were used compared with calculations made with the MsH-PrIH-PrI-Musc model presented in the previous section (Figure 2b and 3b). The K-Beid \pm Qtz \rightarrow illite \pm Kln \pm Qtz \rightarrow Musc sequence observed in the experiments with Musc + Qtz starting material is consistent with the calculated sequence. The proportion of smectite:illite:muscovite can be used to estimate the local composition along the experimental tube (squares and circles in Figure 2a). T-composition diagram calculated by energy minimizing for the system Musc-Kln (+ H₂O) is shown in Figure 3a. The agreement with the experimental results (Figure 3b) is also fair. The

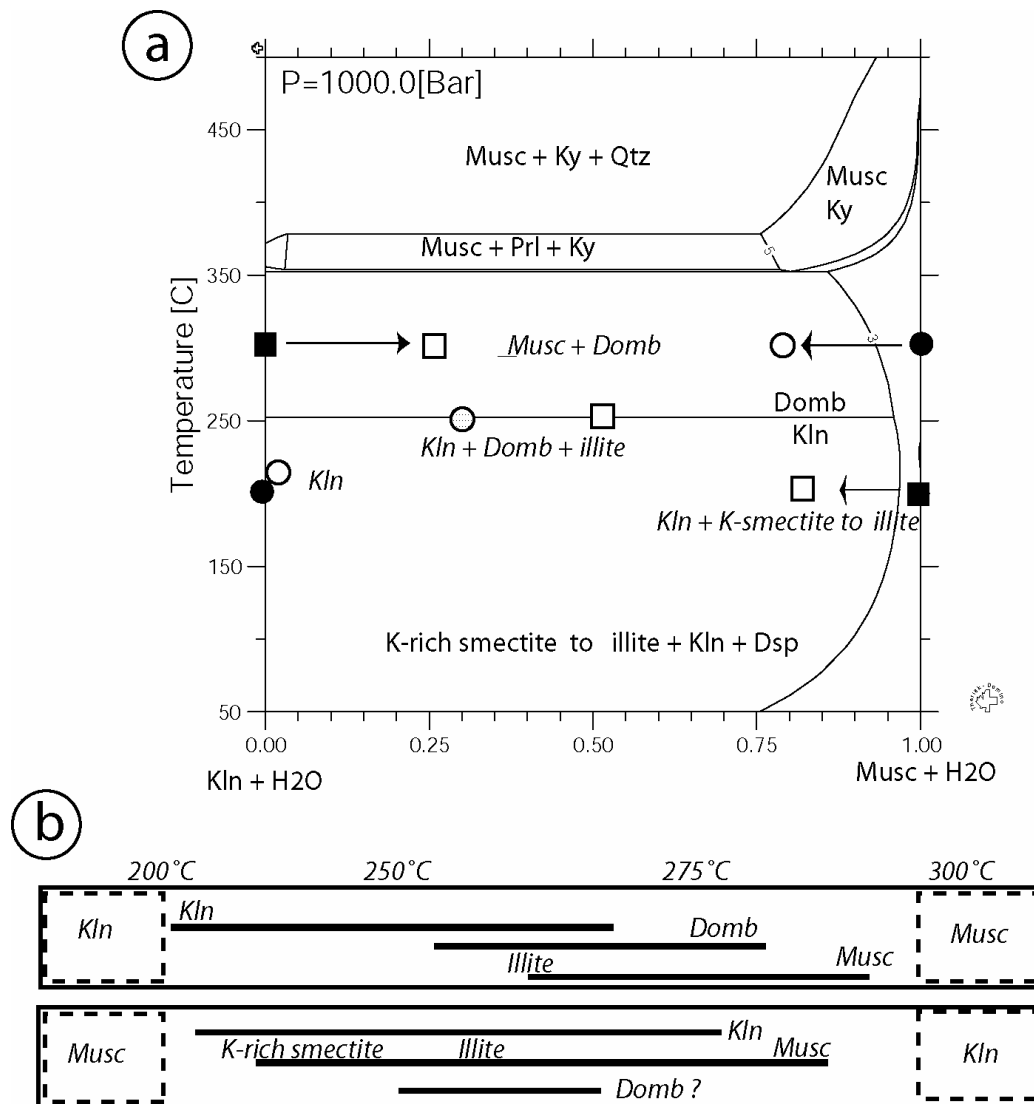
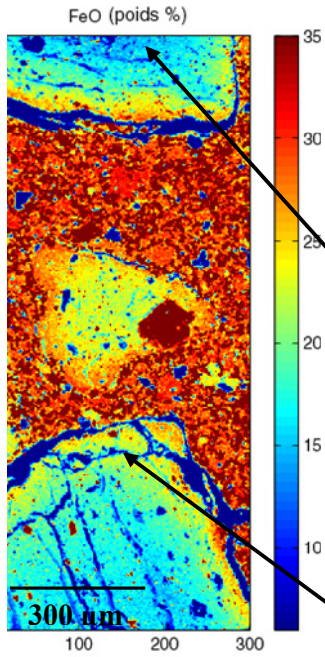


FIGURE 3. a) *T*-composition phase diagram for compositions between *Kln* + H₂O and *Musc* + H₂O, calculated with the same data used for Figure 2. The circles and squares show the evolution of system composition along the tube in experiment 3) and 4), respectively (Figure 3b). b) Results of experiments with *Musc* and *Kln* starting gels.

successive assemblage kaolinite, kaolinite + smectite, illite + dombassite ± kaolinite, *Musc* ± dombassite are consistent with the predicted evolution. The most important disagreement between calculation and experiments concerns diaspore, which is predicted to crystallize although it has not been detected in the experimental products. Calculation of a *T*-composition diagram without diaspore lead to a very different topology compared to that presented in Figure 3b. Therefore, this phase or an equivalent aluminous mineral is required to fit the experimental results. It has been possibly overlooked in the experiments.

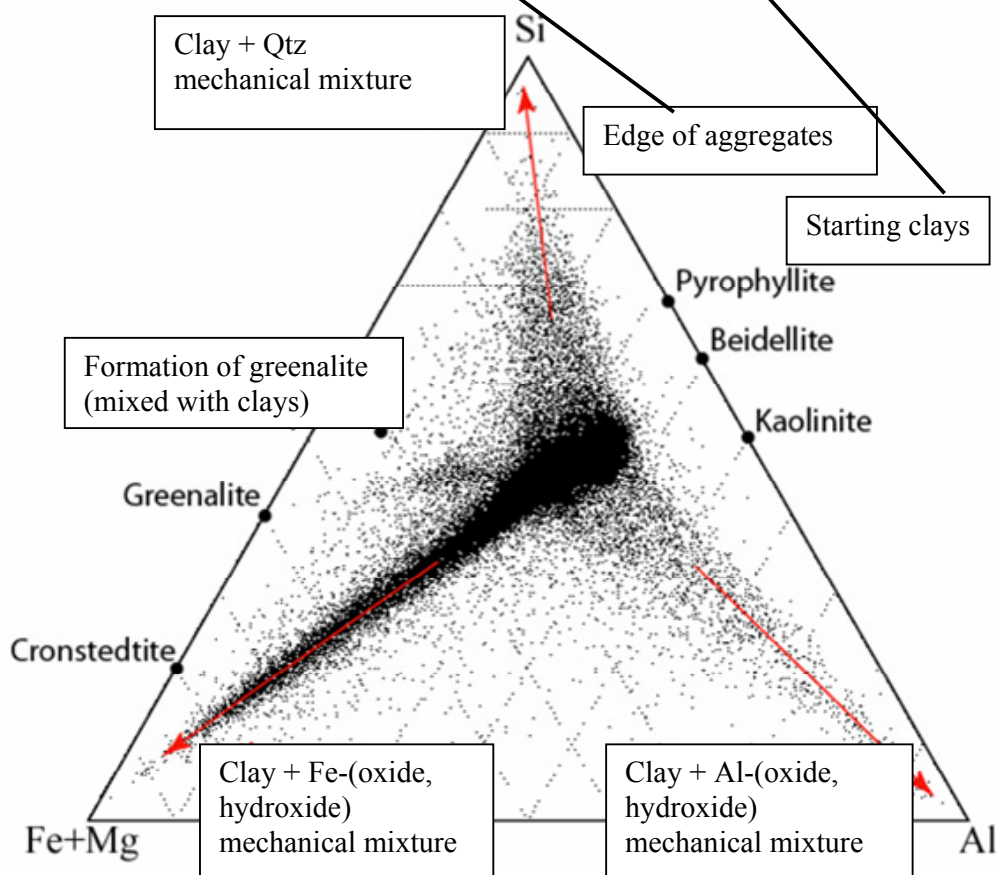
Mapping approach

Application of a multi-equilibrium approach to low grade rocks requires a detailed knowledge of the compositional heterogeneity of phyllosilicates at the micrometric scale. This is best done using quantitative maps of compositions, which can be measured with a microprobe (DeAndrade et al., 2006). The problem of low-temperature rocks is the small size of mineral grains, which can



a

FIGURE 4. a) X-ray map showing the concentration of iron (wt%). Three smectite aggregates can be seen, which are embedded in a fine matrix of smectite + iron powder. A diffusion-like profile of iron can be seen at the edge of aggregates (iron “diffuses” from the matrix into the aggregates). b) Si-Al-Fe+Mg ternary plot of clay pixel compositions (measured every 5 μ m). The trends towards the Si, Al and Fe apexes are due to mechanical mixtures of clays with Qtz, Al- and Fe-oxides or hydroxides. A last trend towards greenalite is observed. These trends evidence the formation of new phases during the ageing of the studied sample.



b

be smaller than the beam size. As a test case, we acquired X-ray maps of composition on part of a thin section made from a mixture of smectite + iron powder, which has been immersed in water for several months at 60°C. Results are reported in Figure 4. Three smectite aggregates are observed in a matrix of fine grained smectite + iron powder. Reaction at the edge of the aggregates is illustrated by the increase of iron concentration at the contact with the iron rich matrix (diffusion-like profil, Figure 4a). The compositional heterogeneity of clays in the studied sample is better evidenced in a Si-Al-Fe ternary (Figure 4b).

All point in this diagram is a pixel analysis (5 μm diameter, one pixel measured every 5 μm). Most pixel analyses concentrate around the starting smectite composition, and the edge of the starting aggregates show compositions richer in Fe. Three trends are observed towards SiO_2 , Al_2O_3 and FeO. They all result from a mixing of clays with quartz, Al- and Fe- oxides or hydroxides, which were undetected by XRD. Quartz and the aluminous phase were not included in the starting mixture. Therefore, these phases formed during the ageing of the sample in water. A last trend is observed from the starting composition towards greenalite, which is mixed with the starting clays. The size of the greenalite grains is probably very small, since no coherent domain with this composition could be identified on the maps of composition.

This example shows that the analytical procedures developed by DeAndrade et al., (2006) and used by Vidal et al. (2006) and Yamato et al. (2007) for chlorite and mica metamorphic samples, can be used to evidence mineral and compositional changes in very low-grade and fine-grained rocks. This suggests that a combination of multi-equilibrium approach with maps of composition should be possible for low-T rocks, and that efforts to constrain reliable and complete solid solution models for smectite are worth to do.

References

- Cathelineau, M., and Nieva, D. (1985). *Contrib. Mineral. Petrol.*, 91, 235-244.
- De Andrade, V., Vidal, O. and Lewin, E. (2006). *Journal of Metamorphic Geology*, 24, 655-668.
- de Capitani, C. (1994). Gleichgewichts-Phasendiagramme: Theorie und Software. Beihefte zum *European Journal of Mineralogy*, 72. Jahrestagung der Deutschen Mineralogischen Gesellschaft, 6,48.
- Green, T.H. (1981). *Contrib. Mineral. Petrol.*, 78: 452-458
- Jiang, W.T., Essene, E.J. and Peacor, D.R. (1990). *Clays and Clay Minerals* 38(3): 225-240.
- Leoni, L., Sartori, F. and Tamponi, M. (1998). *Eur. J. Mineral.*, 10, 1321-1339.
- Loucks, R.R. (1991). *Amer. Mineral.*, 76, 1563-1579.
- Parra T., Vidal, O. and Theye, T. (2005). *American Mineralogist*, 90, 359-370.
- Parra, T., Vidal, O. and Agard, P. (2002). *Contribution to Mineralogy and Petrology*, 143, 706-732.
- Ransom, B. and Helgeson, H.C. (1995). *Am. J. Sci.*, v. 295, p. 245-281.
- Vidal, O., (1997). *European Journal of Mineralogy*, 9, 123-140.
- Vidal, O., DeAndrade, V., Lewin, E., Munoz, M., Parra, T. and Pascarelli, S. (2006). *J. Metam. Geol.*, 24, 669-683
- Vidal, O., Parra T. and Vieillard, P. (2005). *Am. Mineral.*, 90, 359-370
- Vidal, O., Parra, T. and Trotet, F. (2001). *American Journal of Science*, 6, 557-592.